Crystal Structure of *S*-Adenosylhomocysteine Hydrolase from Rat Liver[†,‡]

Yongbo Hu,[§] Junichi Komoto,[§] Yafei Huang,[§] Tomoharu Gomi,[||] Hirofumi Ogawa,[||] Yoshimi Takata,[||] Motoji Fujioka,[||] and Fusao Takusagawa*,[§]

Department of Molecular Biosciences, University of Kansas, Lawrence, Kansas 66045-2106, and Department of Biochemistry, Toyama Medical and Pharmaceutical University, Faculty of Medicine, Sugitani, Toyama 930-0194, Japan

Received February 10, 1999; Revised Manuscript Received April 23, 1999

ABSTRACT: The crystal structure of rat liver *S*-adenosyl-L-homocysteine hydrolase (AdoHcyase, EC 3.3.1.1) which catalyzes the reversible hydrolysis of *S*-adenosylhomocysteine (AdoHcy) has been determined at 2.8 Å resolution. AdoHcyase from rat liver is a tetrameric enzyme with 431 amino acid residues in each identical subunit. The subunit is composed of the catalytic domain, the NAD^+-binding domain, and the small C-terminal domain. Both catalytic and NAD^+-binding domains are folded into an ellipsoid with a typical α/β twisted open sheet structure. The C-terminal section is far from the main body of the subunit and extends into the opposite subunit. An NAD^+ molecule binds to the consensus NAD^+-binding cleft of the NAD^+-binding domain. The peptide folding pattern of the catalytic domain is quite similar to the patterns observed in many methyltransferases. Although the crystal structure does not contain AdoHcy or its analogue, there is a well-formed AdoHcy-binding crevice in the catalytic domain. Without introducing any major structural changes, an AdoHcy molecule can be placed in the catalytic domain. In the structure described here, the catalytic and NAD^+-binding domains are quite far apart from each other. Thus, the enzyme appears to have an "open" conformation in the absence of substrate. It is likely that binding of AdoHcy induces a large conformational change so as to place the ribose moiety of AdoHcy in close proximity to the nicotinamide moiety of NAD^+. A catalytic mechanism of AdoHcyase has been proposed on the basis of this crystal structure. Glu155 acts as a proton acceptor from the O3′-H when the proton of C3′-H is abstracted by NAD^+. His54 or Asp130 acts as a general acid−base catalyst, while Cys194 modulates the oxidation state of the bound NAD^+. The polypeptide folding pattern of the catalytic domain suggests that AdoHcy molecules can travel freely to and from AdoHcyase and methyltransferases to properly regulate methyltransferase activities. We believe that the crystal structure described here can provide insight into the molecular architecture of this important regulatory enzyme.

In biological systems, there are a number of reactions in which a methyl group is transferred from a few types of donor molecules to a wide variety of acceptor molecules. Among the methyl donors, *S*-adenosylmethionine (AdoMet)[1] is the one most widely used, while methyltetrahydrofolate and betaine are involved in far fewer methylation reactions. After transferring the methyl group, AdoMet is converted to *S*-adenosylhomocysteine (AdoHcy), which in turn is hydrolyzed to adenosine (Ado) and homocysteine (Hcy) by the action of *S*-adenosylhomocysteine hydrolase (AdoHcyase, EC 3.3.1.1). The reaction catalyzed by AdoHcyase is reversible, and the equilibrium lies far in the direction of AdoHcy synthesis. Under physiological conditions, however, the removal of both Ado and Hcy is sufficiently rapid that the net reaction proceeds in the direction of hydrolysis (*1*). Ado is removed by Ado deaminase and Ado kinase, and Hcy is used for the synthesis of cysteine and the regeneration of methionine. In mammals, Hcy is produced solely from AdoHcy, and it has been reported recently that an elevated plasma Hcy level is one of the risk factors for coronary heart disease (*2*).

AdoHcy is a potent inhibitor of AdoMet-dependent methyltransferases (*3*−*7*). Since AdoHcyase is the only enzyme involved in AdoHcy metabolism and the reaction it catalyzes is reversible, the activity of AdoHcyase is thought to play a critical role in the control of tissue levels of AdoHcy and, hence, to modulate the activities of various methyltransferases (*8*). Indeed, a variety of inhibitors of this enzyme have been shown to have antiviral activities (*9*−*19*), and to exhibit immunosuppressive (*20*), antiarthritic (*21*, *22*), and antiparasitic (*23*, *24*) properties.

AdoHcyase has been purified from a number of organisms and tissues (*1*, *25*−*37*). The enzymes from all sources are oligomeric proteins with subunits with M_r values of 45000−55000 and isoelectric points of 5.3−6.0. Each subunit contains 1 mol of tightly bound NAD^+. Clones of AdoHcyase have also been obtained from various sources, including rat

[†] The works carried out at the University of Kansas have been supported by NIH Grant GM37233.

[‡] The atomic coordinates have been deposited in the Brookhaven Protein Data Bank (file name 1B3R).

* To whom all correspondence should be addressed: Department of Molecular Biosciences, 3042 Haworth Hall, University of Kansas, Lawrence, KS 66045-2106. Telephone: (785) 864-4727. Fax: (785) 864-5321. E-mail: xraymain@kuhub.cc.ukans.edu.

[§] University of Kansas.

[||] Toyama Medical and Pharmaceutical University.

[1] Abbreviations: Ado, adenosine; AdoHcy, *S*-adenosyl-L-homocysteine; AdoHcyase, *S*-adenosyl-L-homocysteine hydrolase; Hcy, L-homocysteine; AdoMet, *S*-adenosyl-L-methionine; rmsd, root-mean-square deviation; MPD, 2-methyl-2,4-pentanediol; PEG, poly(ethylene glycol).

10.1021/bi990332k CCC: $18.00
Published on Web 06/06/1999

liver (*38*), *Dictyostelium discoideum* (*39*), human placenta (*40*), *Rhodobacter capsulatus* (*41*), *Petroselinum crispum* (*42*), and *Leishmania donovani* (*24*). The deduced amino acid sequences are highly conserved; for example, the amino acid sequence of the rat enzyme is 97% identical with the human enzyme and 52% identical with the *Plasmodium falciparum* enzyme (*43*).

The mechanism of reversible hydrolysis of AdoHcy catalyzed by AdoHcyase has been studied by Palmer and Ableles (*28*, *44*), who showed that AdoHcy and Ado are first oxidized to 3′-keto derivatives by the enzyme-bound NAD^+. This facilitates abstraction of the 4′-proton by an enzyme base, and the resulting carbanion eliminates the 5′-substituent, Hcy or water, to yield 3′-keto-4′,5′-dehydroadenosine. Michael type addition of water or Hcy to this central intermediate, and reduction of 3′-keto by the NADH that is formed, result in the formation of the final product, Ado or AdoHcy. The catalytic mechanism described above is illustrated below.

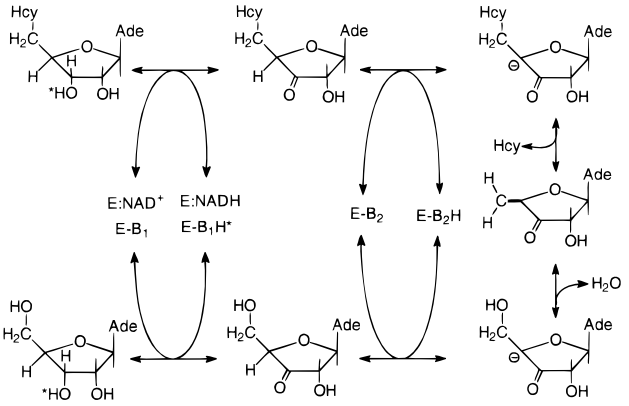

Rat liver AdoHcyase is a tetramer consisting of chemically identical and functionally equivalent subunits (*30*, *45*). Each subunit consisting of 431 amino acid residues contains 1 mol of tightly bound NAD^+. The recombinant enzyme has been produced in *Escherichia coli* using a vector that contains the coding sequence of the cDNA (*46*). Some of the catalytically important amino acid residues have been probed by chemical modification and site-directed mutagenesis studies (*47*−*50*). To better understand the mechanism of action and to provide the bases for designing of potential inhibitors of AdoHcyase, we have carried out a crystallographic study of rat liver AdoHcyase. Here we report the crystal structure determined at 2.8 Å resolution, in which the enzyme takes an open conformation. An X-ray study of human placental AdoHcyase complexed with an inhibitor and taking a closed conformation has recently been published (*51*).

EXPERIMENTAL PROCEDURES

Purification and Crystallization Procedures. AdoHcyase used in this study is the recombinant rat enzyme produced in *E. coli* MV1304 transformed with the pUC118 plasmid that contains the coding sequence of rat AdoHcyase cDNA (*46*). The enzyme was purified to homogeneity from *E. coli* extracts by gel filtration over Sephacryl S-300 and DEAE-cellulose chromatography as described previously. Recombinant AdoHcyase lacks the N-terminal acetyl group but exhibits other structural features similar to those of the liver enzyme (*46*).

Table 1: Experimental Details and Refinement Parameters of Crystal Structure Analyses[a]

Experimental Details	
resolution (Å)	20.0−2.8
no. of crystals	2
no. of reflections measured	280288
no. of unique reflections[b]	56314
% complete	97.5
R_{sym}[c]	0.070
$I/\sigma(I)$[d]	3.41
Refinement Parameters	
no. of residues	1712
no. of NAD^+ molecules	4
no. of water molecules	413
R[e]	0.197
R_{free}	0.268
rmsds	
bonds (Å)	0.011
angles (deg)	1.71
torsion angles (deg)	24.4
mean *B* values	
Cα atoms (Å^3)	19.7
main chain atoms (Å^3)	21.4
all atoms (Å^3)	23.8

[a] Space group $P2_1$ with the following cell dimensions: $a = 94.76$ Å, $b = 134.48$ Å, $c = 102.26$ Å, and $\beta = 114.35°$. The M_r of the subunit is 47 410, with eight subunits in a unit cell; the percentage of solvent content is 60%. [b] Unique reflections in the range between 10.0 Å and the highest resolution. [c] $R_{sym} = \Sigma|I - \langle I\rangle|/\Sigma|I|$. [d] $I/\sigma(I)$ in 3.0−2.8 Å resolution range. [e] $R = \Sigma|F_o - F_c|/\Sigma|F_o|$.

The hanging-drop vapor-diffusion method was employed for crystallization of the enzyme. All crystallization experiments were conducted at 26 °C. Crystals were grown in a buffer containing 50 mM Tris/HCl buffer (pH 6.8), 10 mM $MgCl_2$, and 15% (w/v) PEG 6000 with a protein concentration of 10 mg/mL. The plate-shaped crystals suitable for X-ray diffraction studies (∼0.3 mm × 0.2 mm × 0.1 mm) were grown for 1 day.

Data Measurement. The crystals in a hanging drop were scooped by a nylon loop and were dipped into a cryoprotectant solution containing 20% ethylene glycol, 50 mM Tris/HCl buffer (pH 6.8), 10 mM $MgCl_2$, and 15% (w/v) PEG 6000 for 30 s before they were frozen in liquid nitrogen. The frozen crystals were transferred on a Rigaku RAXIS IIc imaging plate X-ray diffractometer with a rotating anode X-ray generator as an X-ray source (CuKα radiation at 50 kV and 100 mA). The diffraction data were measured up to 2.8 Å resolution at −180 °C. The data were processed with the program DENZO (*52*). Integrated reflections were scaled and reduced with locally developed programs (*53*). The data statistics are given in Table 1.

Structure Determination. The search for good crystals of heavy atom derivatives was not successful. Therefore, the structure determination was carried out by a molecular replacement method. The calculated unit cell volume of 1 187 210 Å^3 suggests that there are four subunits of AdoHcyase in the asymmetric unit, with a V_M of 3.1 Å^3/Da corresponding to a solvent content of 60% (*54*). The four subunits of the tetrameric AdoHcyase should be related with a noncrystallographic 222 symmetry. Initially, the Patterson map was computed and two characteristic features were observed.

(1) The (U 0 W) zone exhibits a pseudo *mm* symmetry whose mirrors are parallel and perpendicular to the crystallographic *a* axis, respectively. This suggests that the two pseudo-2-fold axes are parallel and perpendicular to the crystallographic *a* axis, respectively.

(2) A characteristic peanut-shaped peak that is the second highest in the Patterson map is observed on the coordinate ($^1/_2$, $^1/_2$, 0). This peak indicates that the third 2-fold axis is approximately parallel to the crystallographic *b* axis, and the center of tetrameric AdoHcyase is located at ($^1/_4$, *y*, 0).

To confirm this conclusion, a known tetrameric structure (glycine *N*-methyltransferase) was placed at ($^1/_4$, *y*, 0) in the AdoHcyase unit cell, and the molecule was oriented so that the noncrystallographic 2-fold axes were along the *a* and *b* axes and perpendicular to the *ab* plane, respectively. The calculated Patterson map of the model rotated by 1.5° around the *a* axis exhibits an *mm* symmetry in the (U 0 W) zone as well as a peanut-shaped peak at ($^1/_2$, $^1/_2$, 0).

A search of the PDB files indicates that the structures of 36 unique NAD^+-binding proteins have been deposited. These 36 coordinates were downloaded into our computer. The NAD^+-binding domains were abstracted from the coordinate files. All of the amino acid residues were converted to alanines, and then large loop sections were deleted from the models. These 36 polyalanine models were utilized for molecular replacement searches. All molecular replacement calculations were carried out by using the program X-PLOR (*55*). The highest 120 solutions of each rotation search were employed in the Patterson correlation (PC) refinement (*56*). A solution with the highest peak after PC refinement was put into the translation search. The tetrameric structure was computed from the subunit coordinate deduced from the translation search by applying the noncrystallographic 222 symmetry. In the calculation, the *y* coordinate of the subunit was adjusted to form a contact tetramer around the coordinate ($^1/_4$, 0, 0). The subunit coordinates of the resulting tetrameric structures were refined by a rigid-body least-squares method. The $2F_o - F_c$ map computed with the phases from the NAD^+-binding domain of formate dehydrogenase [PDB file name 2NAD (*57*)] exhibited the electron density peaks not only of the main chain of the NAD^+-binding domain but also of the side chains. The map also showed some electron density peaks of the α-helices and *β*-strands of the catalytic domain. Thus, this model was judged to represent the correct structure.

The initial model was built on an SGI workstation using the program TOM/FRODO (*58*, *59*). The model was refined with the POSITIONAL protocol and then with the simulated annealing procedure of X-PLOR (*55*). In the first several cycles of refinement, noncrystallographic symmetry restraints were applied. Models were rebuilt where necessary, and previously undefined residues were built into the electron density maps. After multiple cycles of model building and refinement, four bound NAD^+ molecules and all the residues except for three amino acid residues of the N-terminus were built into the electron density map. Refinement of isotropic temperature factors for individual atoms was carried out by the individual *B*-factor refinement procedure of X-PLOR using bond and angle restraints. During the final refinement stage, well-defined residual electron density peaks in difference maps were assigned to water molecules if peaks were

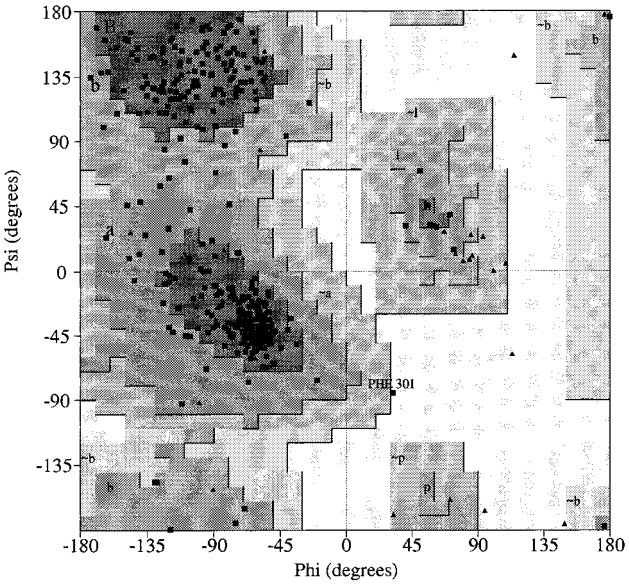

FIGURE 1: Ramachandran plot of the main chain dihedral angles for the final atomic model (subunit A). Glycine residues are denoted as triangles.

able to bind the protein molecules with hydrogen bonds. The final crystallographic *R*-factor is 0.197 for all data (no *σ* cutoff) from 8.0 to 2.8 Å resolution. The R_{free} for randomly selected 5% data is 0.268 (*60*). The coordinates have been deposited in the Brookhaven Protein Data Bank (file name 1B3R).

Although the search model (NAD^+-binding domain) used in this study is relatively small, a molecular replacement method has worked in determining the relatively large unknown structure. It is noted that this is a special case. As will be discussed later, the NAD^+-binding domains form the core of the tetrameric enzyme and their temperature factors are much smaller than those of the catalytic domains. Therefore, the NAD^+-binding domains contribute largely in determining the phase angles and the amplitudes of the structure factors. It is noted that Turner et al. (*51*) state that the highest degree of structural homology of the structure of human AdoHcyase was found with formate dehydrogenase.

RESULTS

Overall Structure. The crystallographic refinement parameters (Table 1), final $2F_o - F_c$ maps, Ramachandran plot (Figure 1), and conformational analysis by PROCHECK (*61*) indicate that the structure of AdoHcyase has been determined successfully. AdoHcyase consists of four subunits related by a pseudo-222 symmetry (Figure 2). The four subunits are denoted subunits A−D. Although the four subunits are crystallographically independent, the subunits are structurally very similar. The rmsds of the Cα among the subunit structures related by a pseudo-222-fold symmetry are less than 0.42 Å (Table 2). For simplicity, the following description mainly refers to subunit A.

Structure of the Subunit. The AdoHcyase subunit is composed of three domains, with the peptide chain organized into 16 α-helices and 15 *β*-strands as determined with the program PROCHECK (Figure 3). The three domains are denoted the catalytic domain (residues 1−181 and 352−402), the NAD^+-binding domain (residues 182−351), and the

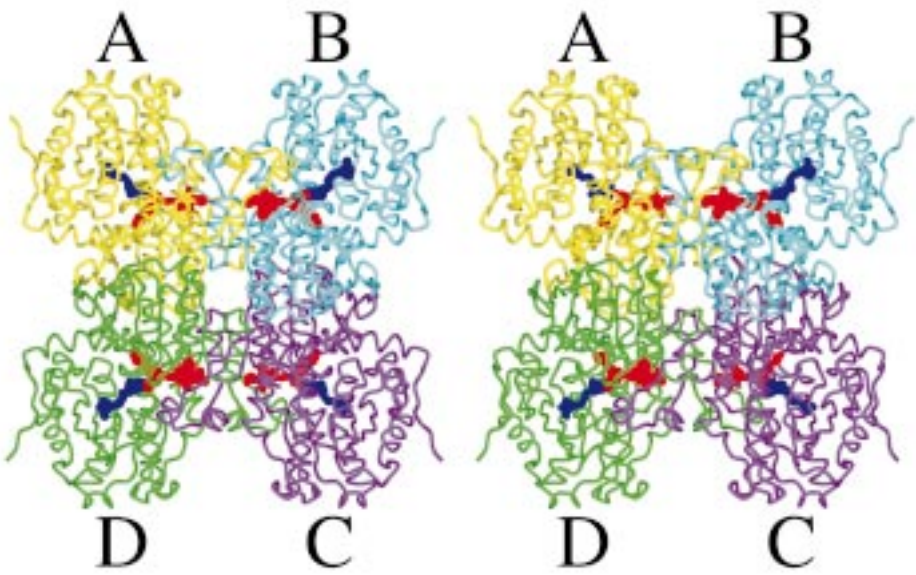

FIGURE 2: Tetrameric structure of AdoHcyase. Subunits A−D related by a pseudo-222 symmetry are denoted by letters and are yellow, cyan, magenta, and green, respectively. Four tightly bound NAD^+ molecules and four AdoHcy molecules deduced from a modeling study are illustrated as red and blue sticks, respectively.

Table 2: Root-Mean-Square Deviations (Å) between Two Structures

structure 1	structure 2	Cα (428 atoms)	main chain (1711 atoms)	all (4023 atoms)
subunit A	subunit B	0.42	0.45	0.76
subunit A	subunit C	0.42	0.45	0.76
subunit A	subunit D	0.08	0.11	0.21
subunit B	subunit C	0.08	0.10	0.18
subunit B	subunit D	0.40	0.43	0.74
subunit C	subunit D	0.40	0.43	0.75

C-terminal domain (residues 403−431) (Figure 4). The small C-terminal domain that is composed of random coil−two-turn α-helix−random coil is apart from the main body of the subunit and extends to the adjacent subunit B. The catalytic and NAD^+-binding domains are each folded into an ellipsoid with a typical α/β twisted open sheet structure. A relatively wide but short β-sheet is formed in the center of each ellipsoidal domain. The two domains are connected at the ellipsoidal pole sections by exchanging a pair of relatively long α-helices (αN of the catalytic domain and αG of the NAD^+-binding domain). Consequently, the subunit of AdoHcyase is shaped like a "fat U". It is noted that the longest α-helix αG in the catalytic domain that might serve as a molecular hinge is slightly bent (∼15°) in the middle. In the catalytic domain, the β-sheet is composed of seven parallel β-strands, and is covered by four and three α-helices at either side. The β-sheet found in the NAD^+-binding domain is composed of five parallel β-strands and a pair of antiparallel β-strands. The β-sheet is covered with three and two α-helices, respectively. As shown in Figure 3, the peptide folding pattern of the NAD^+-binding domain is quite similar to that of the catalytic domain. There is a large cleft between the catalytic domain and the NAD^+-binding domain. The β-sheet tips (C-terminal ends) of the catalytic domain and the NAD^+-binding domain point to each other across the cleft. An NAD^+ molecule lies in a crevice between the tips of β7 and β10 with the pyrophosphate group straddling the β-sheet and the two ends on the opposite sides of the β-sheet. The NAD^+ molecule is tightly held by hydrophobic interactions and by hydrogen bonds [O1PN(NAD)···N(Val223), O7N(NAD)···ND2(Asn345), N7N(NAD)···O(Ile298), N7N-(NAD)···OD1(Asn345), O1PA(NAD)···OH(Tyr429B), O2′A-(NAD)···OE1(Glu242), O3′A(NAD)···OE2(Glu242), O2′A-(NAD)···NZ(Lys425B), and O3′A(NAD)···NZ(Lys425B)] (Figures 5A and 6A). It is noted that Lys425 and Tyr429 from the adjacent subunit B participate in the hydrogen bonds. The nicotinamide moiety of NAD^+ is positioned near the bottom of the "fat U" and faces the β-strands of the catalytic domain, whereas the adenine moiety is far from the catalytic domain.

Tetrameric Structure. Four subunits are connected around a pseudo-222 symmetry to form a tetramer (Figure 2). The four NAD^+-binding domains are located near the center of the tetramer, and are tightly connected with each other by both polar and nonpolar interactions. The catalytic domains are placed far from the center of the tetramer, and therefore, they have little interaction with each other. The tetrameric structure indicates that the catalytic domains are more mobile compared with the NAD^+-binding domains. Indeed, the average temperature factor of the catalytic domain is significantly higher than that of the NAD^+-binding domain (29.8 vs 10.2 $Å^2$). In the small C-terminal domain, the two-turn α-helix αP (residues 409−416) participates in forming the adenine pocket of the NAD^+ bound to subunit B (Figure 4). The hydrophilic C-terminus extends into the central channel as described below and interacts with the phosphate and ribose moieties of the NAD^+ bound to subunit B. Formation of the tetramer creates a unique channel structure (∼10 Å × 10 Å × 50 Å) that passes through the center of the tetramer (Figure 7). The channel is built with four sets of αG−αI helices of the NAD^+-binding domains. The interior surface of the channel is covered with four sets of 13 hydrophilic amino acid residues from the three α-helices (Lys187, Tyr192, and Arg195 from αG, Tyr220, Asp222, Lys225, Gln229, and Arg232 from αH, and Asp244, Asn247, Gln250, Glu254, and Glu256 from αI). The hydrophilic C-terminus (Asp427, His428,

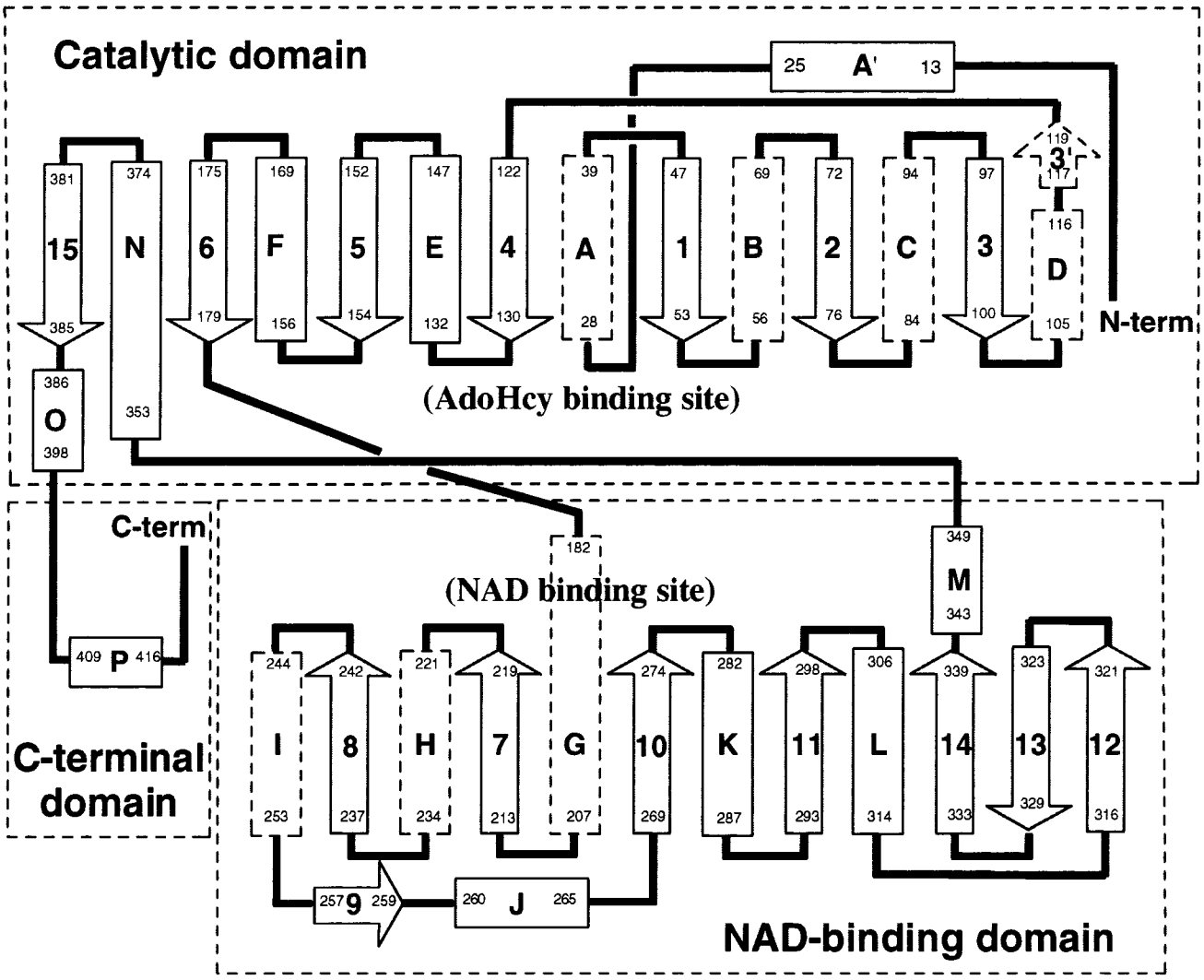

FIGURE 3: Topology diagram showing the catalytic, NAD^+-binding, and C-terminal domains. The α-helices and β-strands are denoted by rectangles and arrows, respectively. The small numbers in the rectangles and arrows represent amino acid residue numbers. The helices with dotted lines are under the β-sheet.

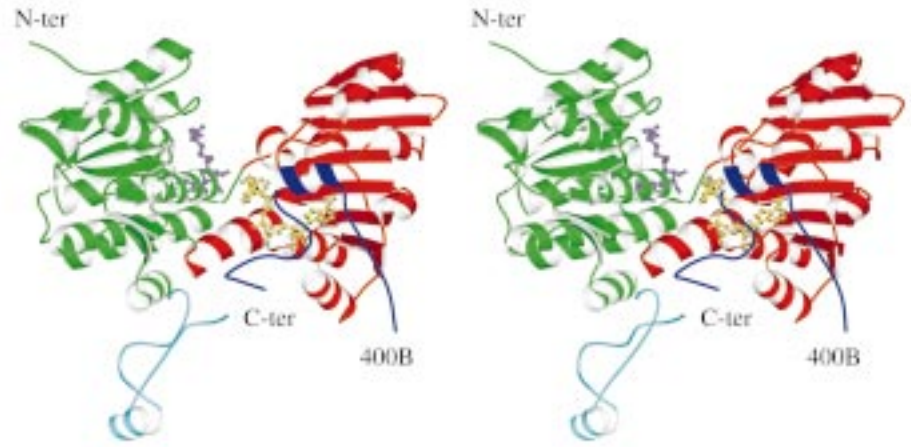

FIGURE 4: Ribbon drawing of a single subunit of AdoHcyase showing three domains: the catalytic domain (green), the NAD^+-binding domain (red), and the C-terminal domain (cyan). The C-terminal domain from subunit B is blue. The bound NAD^+ molecule and the AdoHcy molecule deduced from a modeling study are depicted yellow and magenta sticks, respectively.

Tyr429, Arg430, and Tyr431) extends into the channel. These amino acid residues are connected to each other by hydrogen bonds and salt linkages. Two NAD^+ molecules are placed at the edge of the channel at the both ends. Twenty-four well-defined water molecules are found in the channel. The exact biological role of this unique channel structure is unknown.

AdoHcy Binding Model. The peptide folding pattern of the catalytic domain is quite similar to the folding pattern of catalytic domains of various AdoMet-dependent methyl-

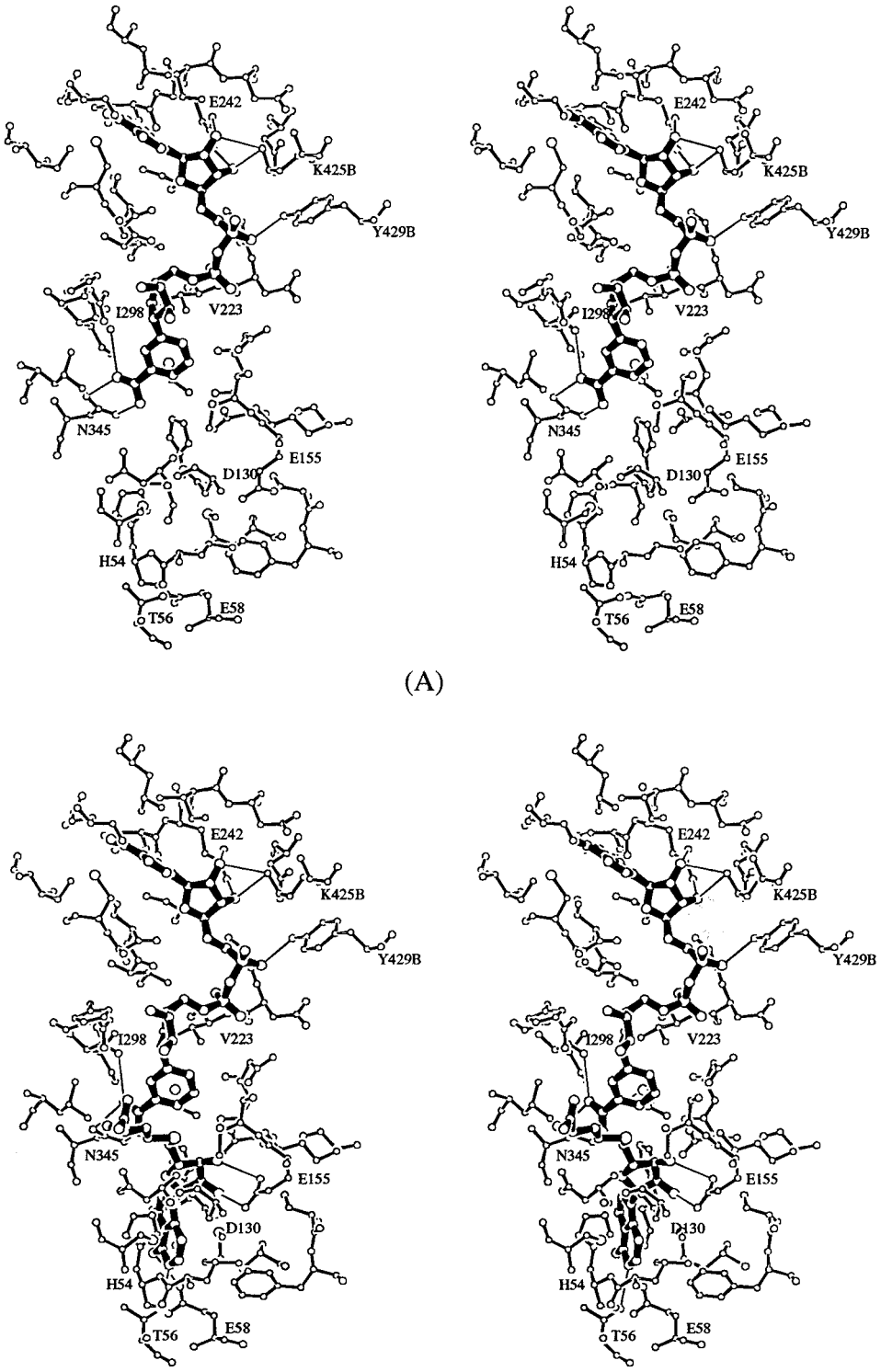

FIGURE 5: Geometries of the NAD^+ and AdoHcy binding sites: (A) NAD^+-binding site from the X-ray study and (B) NAD^+- and AdoHcy-binding sites from the modeling. In the X-ray structure, a well-defined AdoHcy binding site is seen in the bottom of the NAD^+-binding site. It is noted that an AdoHcy molecule is fitted into the X-ray structure without any major conformational changes. Possible hydrogen bonds are depicted as thin lines. NAD^+ and AdoHcy molecules are depicted as thin solid bonds.

transferases (*62*−*70*). Furthermore, there is a well-formed crevice between strands β1 and β4 as observed in methyltransferases. A hydrophobic pocket-like structure is formed at the end of the crevice (Figure 5b). An AdoHcy molecule was introduced into the crevice to place its adenine moiety in the hydrophobic pocket and to form hydrogen bonds between the adenine ring and the sounding amino acid residues. The model crystal structure was manually adjusted on a graphic workstation and refined using the POSITIONAL refinement protocol with the program X-PLOR. The X-ray contribution part, xref, was excluded in the calculation, and no water molecule was added in the model. Although the side chains of amino acid residues moved slightly by refinement, the refined model structure was essentially the

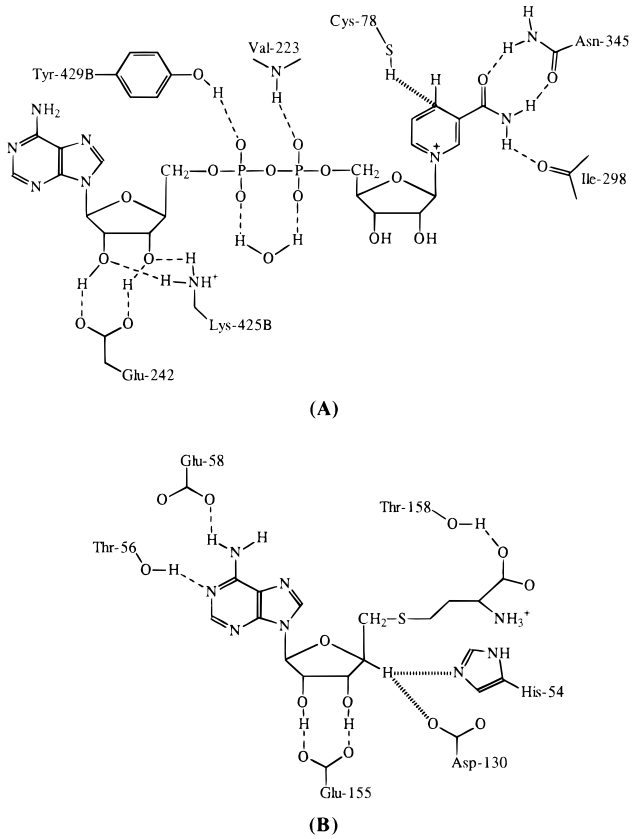

FIGURE 6: Schematic diagrams of interactions of (A) NAD^+ in the active site and (B) AdoHcy in the model structure. The possible hydrogen bonds are depicted as dashed lines. The weak interactions that are important for the catalysis are depicted as thick dashed lines.

same as the X-ray structure with an AdoHcy, indicating that an AdoHcy molecule can fit into the catalytic site without any major conformational changes in the AdoHcyase structure (Figure 5B). Thr56 and Glu58 hydrogen bond to the adenine ring, and Glu155 recognizes the ribose moiety by a pair of hydrogen bonds (Figure 6B). Polar amino acid residues, His54 and Asp130, which could serve as a general base in the abstraction of a 4′-proton of AdoHcy, are seen near the ribose moiety. However, it should be noted that the ribose moiety of AdoHcy is quite distant from the nicotinamide moiety of NAD^+ [for example, C3′(AdoHcy)···C4-(NAD) = 6.3 Å] (Figure 5B).

DISCUSSION

The crystallographic study described in this report provides information about the secondary, tertiary, and quaternary structures of rat liver AdoHcyase, and the amino acid residues possibly involved in catalysis and NAD^+ binding have been identified.

In open twisted α/β structures, it is known that a substrate binds to the crevice formed between two β-strands that are joined by a crossover connection (see, for example, ref *71*). The structure of AdoHcyase presented here has two large domains, each of which is composed of a typical open twisted α/β structure. A tightly bound NAD^+ molecule is found in the crevice of one of the domains. Amino acid sequence analysis indicated that the region from Lys213 to Asp244 conformed to the "fingerprint" sequence of the dinucleotide-binding domain with the sequence GXGXXG at positions 219−224 (*38*). Indeed, in this crystal structure, an NAD^+ molecule binds at the tips (C-terminal ends) of β7 and β10, where the strand order is reversed. The two loops connecting β7 and αH, and β10 and αK, form the NAD^+-binding cleft. The pyrophosphate of NAD^+ binds to the central region of the domain straddling the β-sheet. The adenine moiety lies on strands β7 and β8, while the nicotinamide is on the other side of strands β10 and β11. The consensus hydrogen bond that connects the 2′-OH of adenosine ribose and an acidic amino acid residue (Asp or Glu) is observed between 2′-OH and the carboxyl group of Glu242. Previously, we showed that the mutagenic change of Asp244 to a glutamate resulted in a large reduction in the affinity for NAD^+ (*47*). Thus, the NAD^+-binding cleft is precisely at the position predicted from the general sequence consensus (*72*).

Although the crystal structure does not contain AdoHcy or its analogue, there is a well-formed crevice between strands β1 and β4 in the catalytic domain. A simple modeling study indicates that an AdoHcy molecule can fit the crevice without introducing major structural changes. In the model structure, AdoHcy binds to the catalytic domain with its adenine moiety inserted into the deep cavity. This is consistent with the results of previous spectrophotometric and solvent perturbation studies which showed that the adenine existed in a hydrophobic environment (*73*). The Hcy and ribose are exposed in the solvent channel. Aksamit et al. (*48*) have proposed from site-directed mutagenesis studies that Cys78 is located near the AdoHcy-binding site, although not directly involved in the catalytic reaction. The crystal structure indicates the occurrence of Cys78 in the loop between β2 and αC, which is near the binding site of the adenine moiety of AdoHcy. Yuan et al. (*50*) have shown that Cys194 occurs in the catalytic center and suggested that it plays an important role in maintaining the 3′-OH reduction potential for the effective release of the reaction products and regeneration of the active form (NAD^+ form) of the enzyme. The S atom of C194 and the C4 of nicotinamide are at a distance of 3.8 Å. Although it is slightly long, if the distance indicates partial reduction of bound NAD^+ by Cys194, the results of Yuen et al. (*50*) are consistent with the reaction mechanism proposed below.

In the structure of rat liver AdoHcyase obtained here, the catalytic and NAD^+-binding domains are apart from each other. This "open" structure is in contrast with the "closed" structure reported for human AdoHcyase complexed with a substrate analogue, 2′-hydroxyl-3′-ketocyclopent-4′-enyladenine (*51*). Thus, it is reasonable to assume that the large cleft between the two domains is closed upon binding of the substrate to bring NAD^+ and substrate into close proximity. Since the NAD^+-binding domains are attached together at the center of the tetramer, the catalytic domain should move toward the former. This movement would place the C3′-H of AdoHcy very close to the nicotinamide C4 of NAD^+. It is most likely that rotation occurs at the N-terminal end of the long αG that connects the catalytic domain to the NAD^+-binding domain. For example, if the torsion angle of the Cα−N bond of Thr184 in αG is changed from −69° to −87°, the cleft is closed and AdoHcy moves toward the NAD^+ (Figure 8). Such a conformational change could move some of atoms on the surface of the catalytic domain more than 10 Å from their original sites. Since the small C-terminal domain bridges the mobile catalytic domain and the station-

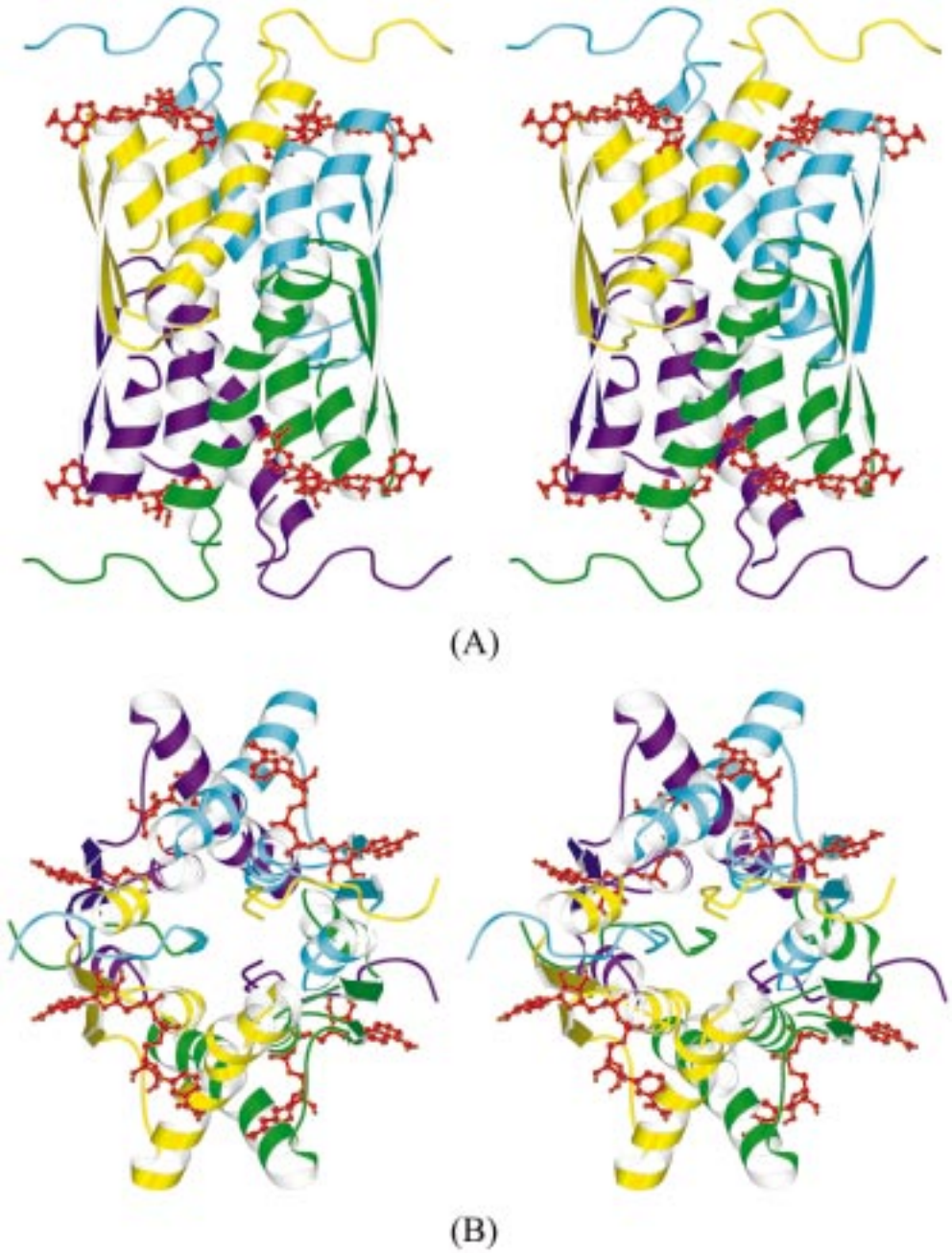

FIGURE 7: Unique channel structure composed of four sets of three α-helices (αG−αI) that passes through the center of the tetramer: (A) a side view of the channel and (B) a view down the channel. The dimension of the channel is ~10 Å × 10 Å × 50 Å. The diagram contains four sets of residues 180−256 and the C-terminal tails (420−431) from the four subunits (yellow, cyan, magenta, and green). Four NAD^+ molecules on the edges of the channel are red. It is noted that the C-termini hang into the channel as if they cork the entrances of the channel.

ary NAD^+-binding domain of the adjacent subunit, a slight movement of the C-terminal domain upon AdoHcy binding might trigger a large conformational change of the catalytic domain. Substrate-induced conformational change is a well-established phenomenon (see, for example, ref *74*).

As indicated by the temperature parameters of atoms, the catalytic domain is quite mobile, whereas the NAD^+-binding domain and the small C-terminal domain are less mobile. The high mobility of the catalytic domain is due to the unique architecture of the tetramer. As described in the previous section, a channel is formed in the center of the tetramer (Figure 7). This channel structure not only provides a strong core framework but also offers mobility to the catalytic domains. If the NAD^+-binding domains were tightly connected to each other without creating the hollow channel, the catalytic domains would lose their mobility since they would be close to each other in the tetrameric structure. If, on the other hand, the NAD^+-binding domains were less tightly connected so a high mobility of the catalytic domains was maintained, the enzyme would not be able to keep the tetrameric structure. In the tetramer, the small C-terminal domains are exchanged between the adjacent subunits and form part of the NAD^+-binding sites. Therefore, the enzyme must at least be a dimer to properly form the NAD^+-binding sites. However, the dimer structure cannot provide a strong rigid core framework. Formation of the tetramer allows AdoHcyase to build a strong and rigid molecular framework as well as flexible catalytic sites. The hydrophilic C-termini

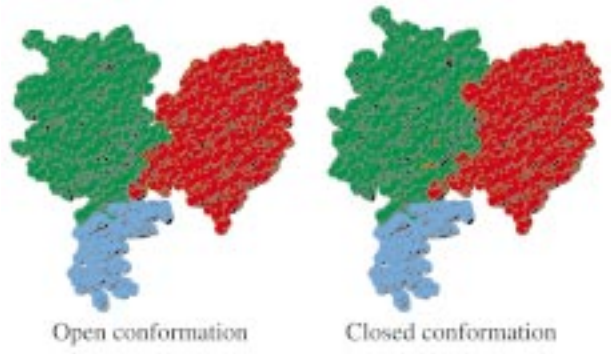

FIGURE 8: "Open" and "closed" structures of the AdoHcyase. The catalytic domain, NAD^+-binding domain, and small C-terminal domain are green, red, and cyan, respectively. The closed structure is generated by rotating the Cα−N bond of Thr184 from −69° to −87°.

might cork the entrances of the channel to prevent a possible disruption of the channel structure caused by any disturbance inside the channel such as metal ion binding. It is noted that catalytic domains could move in other open−closed structures without the channel (see, for example, ref *74*).

Interestingly, the length (~50 Å) of the channel observed in this structure is similar to those observed in the channel-forming transmembrane proteins, such as bacteriorhodopsin (*75*, *76*), K^+ channel (*77*), and *E. coli* OmpF porins (*78*). The diameter of the channel is quite wide (~10 Å) and comparable to those of *E. coli* OmpF porins.

On the basis of the crystal structure and modeling study, the mechanism of hydrolysis of AdoHcy could be visualized as follows. The adenosine moiety of AdoHcy is held to the enzyme by hydrogen bonds [N1A···OG1(Thr56), N6A···OE1(Glu58), O2′···OE1(Glu155), and O3′···OE2(Glu155)]. Upon binding of AdoHcy, the catalytic domain moves toward the NAD^+-binding domain so the C3′-H is placed near the C4 of nicotinamide of NAD^+. The OE2 of Glu155 serves as a base to accept the proton from O3′-H. The HS group of Cys194 would move away from the C4 of NAD^+ by rotating the Cβ−S bond. This would bring the NAD^+ to a higher oxidation state and facilitate abstraction of the C3′-H of the substrate. In the model structure, Asp130 and His54 are near the C4′ of AdoHcy [C4′···OD1(Asp130) = 3.7 Å, C4′···NE2(His54) = 3.9 Å]. Thus, it is highly likely that either Asp130 or His54 acts as a base to directly abstract the proton from C4′ of the substrate. The resulting carbanion then eliminates Hcy to form the 3′-keto-4′,5′-dehydroadenosine intermediate. After addition of OH^- to C5′ of the intermediate, the protonated base (Asp130 or His54) returns a proton to C4′, and the Cβ−S bond rotation allows approach of the Cys194 SH group to NADH. Reduction of the 3′-keto group by the enzyme-bound NADH and the protonated Glu155 completes the hydrolysis. A schematic representation of the mechanism is illustrated below.

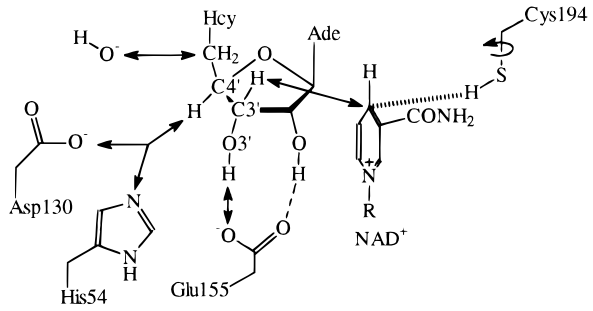

In contrast, Turner et al. (*51*) have proposed that Lys185 is the proton acceptor of O3′-H and a water molecule activated by Asp130 and His54 abstracts the proton of C4′-H.

It has been postulated that AdoHcyase and AdoMet-dependent methyltransferases would have a common structure at the substrate binding sites since AdoHcy is an effective product inhibitor of methyltransferases. In the AdoHcy-binding domain of AdoHcyase, the peptide folding pattern from helix αA (residues 28−39) to helix αF (residues 156−169) is exactly the same as the pattern seen in methyltransferases of known structures (*68*, *79*), although the folding pattern of the C-terminal edge (β6, β7, and αF) is slightly different. The number of amino acid residues composing the AdoHcy-binding domain of AdoHcyase (181) is also quite similar to that of the catalytic domain of methyltransferase [for example, the AdoMet-binding domain of glycine *N*-methyltransferase has 178 residues (*68*)]. In a

Table 3: Summary of the Crystallographic Data of Rat and Human AdoHcyases

	rat AdoHcyase (this study)	human AdoHcyase
crystallization conditions	15% PEG 6000, 10 mM $MgCl_2$, and 50 mM Tris/HCl (pH 6.8)	12% PEG 4000, 20% 2-propanol, 200 mM ammonium acetate, and 100 mM citrate buffer (pH 5.6)
space group	$P2_1$	$C222$
unit cell dimension	a = 94.76 Å, b = 134.48 Å, c = 102.26 Å, β = 114.35°, and V = 1 187 210 Å^3	a^b = 96.2 Å, b = 173.6 Å, c = 142.9 Å, and V = 2 386 476 Å^3
	a^a = 94.76 Å, b = 186.62 Å, c = 134.48 Å, β = 93.21°, and V = 2 374 428 Å^3	a^c = 91.93 Å, b = 168.02 Å, c = 137.77 Å, and V = 2 128 006 Å^3
no. of subunits in asymmetric unit	4	2
structure determination method	molecular replacement with NAD-binding structures	MAD with SeMets
resolution (Å)	8.0−2.8	50−2.8
no. of independent reflections used	56314 (all data)	49579 (all data)
bulk solvent correction	not applied	applied
R, R_{free}	0.197, 0.268	0.222, 0.243
rmsd for bonds (Å), rmsd for angles (deg)	0.011, 1.71	0.008, 1.68
most favorable regions in Ramachandran plot (%)[d]	87.7	83.0
cofactor, inhibitor	NAD^+, no inhibitor	NADH, DHCaA
conformation	open	closed

[a] Pseudo-*C*222 cell. [b] From ref *83*. [c] From ref *51*. [d] According to the program PROCHECK (*61*).

methyltransferase, AdoMet binds on the tips of β-strands that are joined by a crossover connection. AdoHcyase binds AdoHcy at a similar part of the enzyme. It should be noted, however, that consensus amino acid sequences observed at the AdoMet-binding site of methyltransferases are not observed in AdoHcyase.

It is interesting to compare the structures of AdoHcyase and related enzymes. The AdoMet-binding pocket of AdoMet synthetase, which catalyzes the synthesis of AdoMet from methionine and ATP, is structurally quite different from the AdoMet- and AdoHcy-binding pockets of methyltransferases and AdoHcyase (*80*). Methionine synthase (*81*) and methionine repressor (*82*), whose biological activities are regulated by AdoMet, do not have the polypeptide folding pattern seen in methyltransferases and AdoHcyase. It appears that AdoMet- and AdoHcy-binding pockets can be constructed in various ways to support different biological functions. For example, the AdoMet binding pocket of AdoMet synthetase is designed to release the AdoMet that is formed (low-affinity), while that of methyltransferase is constructed to capture cytosolic AdoMet (high-affinity) and to convert it to AdoHcy. AdoHcyase and methyltransferases have a similar structural motif at the substrate binding sites that may be helpful for AdoHcy in traveling freely to and from these enzymes to regulate methyl transfer reactions.

Because the atomic coordinate data of human AdoHcyase have not been released, it is not possible to compare the structures of rat and human enzymes at the atomic level. However, it is interesting to compare their crystallographic data. As summarized in Table 3, both enzymes are crystallized in related space groups. To directly compare the unit cell dimensions, the monoclinic unit cell ($P2_1$ space group) of rat AdoHcyase is converted to a nonprimitive pseudo-orthorhombic unit cell (pseudo-$C222$ space group). The resulted pseudo orthorhombic unit cell dimensions are similar to those in the preliminary report of human AdoHcyase (*83*). Especially the cell volumes of both enzymes are the same (2.37×10^6 vs 2.38×10^6 Å^3). Although the crystallization, data collection, and structure determination of rat and human AdoHcyases have been carried out independently, the refinement parameters are quite similar to each other.

REFERENCES

1. Richards, H. H., Chiang, P. K., and Cantoni, G. L. (1978) *J. Biol. Chem. 253*, 4476−4480.
2. Nygard, O., Nordrehaug, J. E., Refsum, H., Ueland, P. M., Farstad, M., and Vollset, S. E. (1997) *N. Engl. J. Med. 337*, 230−236.
3. Hurwitz, J., Gold, M., and Anders, M. (1964) *J. Biol. Chem. 239*, 3474−3482.
4. Deguchi, T., and Barchas, J. (1971) *J. Biol. Chem. 246*, 3175−3181.
5. Coward, J. K., Slisz, E. P., and Wu, F. Y.-H. (1973) *Biochemistry 12*, 2291−2297.
6. Pugh, C. S. G., Borchardt, R. T., and Stone, H. O. (1977) *Biochemistry 16*, 3928−3932.
7. Hasebe, M., Mckee, J. G., and Borchardt, R. T. (1989) *Antimicrob. Agents Chemother. 33*, 828−834.
8. Cantoni, G. L. (1986) in *Biological Methylation and Drug Design* (Borchardt, R. T., Creveling, C. R., and Ueland, P. M., Eds.) pp 227−238, Humana Press, Clifton, NJ.
9. Hershfield, M. S. (1979) *J. Biol. Chem. 254*, 22−25.
10. Ransohoff, R. M., Narayan, P., Ayer, D. F., Rottman, F. M., and Nilson, T. W. (1987) *Antiviral Res. 7*, 317−327.
11. De Clercq, E. (1987) *Biochem. Pharmacol. 36*, 2567−2575.
12. Keller, B. T., and Borchardt, R. T. (1988) in *Antiviral Drug Development* (De Clercq, E., and Walker, R. T., Eds.) pp 123−138, Plenum, New York.
13. McCarthy, J. R., Jarri, E. T., Matthews, D. P., Edwards, M. L., Prakash, N. J., Bowlin, T. L., Mehdi, S., Sunkara, P. S., and Bey, P. (1989) *J. Am. Chem. Soc. 111*, 1127−1128.
14. Kramer, D. L., Porter, C. W., Borchardt, R. T., and Sufrin, J. R. (1990) *Cancer Res. 50*, 3838−3842.
15. Wolfe, M. S., and Borchardt, R. T. (1991) *J. Med. Chem. 34*, 1521−1530.
16. Patil, S. D., Schneller, S. W., Hosoya, M., Snoeck, R., Andrei, G., Balzarini, J., and De Clercq, E. (1992) *J. Med. Chem. 35*, 3372−3377.
17. Liu, S., Wnuk, S. F., Yuan, C., Robins, M. J., and Borchardt, R. T. (1993) *J. Med. Chem. 36*, 883−887.
18. Villalon, M. D. G., Gil-Fernandez, C., and De Clercq, E. (1993) *Antiviral Res. 20*, 131−144.
19. Wnuk, S. F., Yuan, C. S., Borchardt, R. T., Balzarini, J., De Clercq, E., and Robins, M. J. (1994) *J. Med. Chem. 37*, 3579−3587.
20. Wolos, J. A., Frondorf, K. A., and Esser, R. E. (1993) *J. Immunol. 151*, 526−534.
21. Wolos, J. A., Frondorf, K. A., Babcock, G. F., Stripp, S. A., and Bowlin, T. L. (1993) *Cell. Immunol. 149*, 402−408.
22. Wolos, J. A., Frondorf, K. A., Davis, G. F., Jarvi, E. T., McCarthy, J. R., and Bowlin, T. L. (1993) *J. Immunol. 150*, 3264−3273.
23. Bitonti, A. J., Baumann, J., Jarvi, T., McCarthy, J. R., and McCann, P. P. (1990) *Biochem. Pharmacol. 40*, 601−606.
24. Henderson, D. M., Hanson, S., Allen, T., Wilson, K., Coulter-Karis, D. E., Greenberg, M. L., Hershfield, M. S., and Ullman, B. (1992) *Mol. Biochem. Parasitol. 53*, 169−183.
25. Poulton, J. E., and Butt, V. S. (1976) *Arch. Biochem. Biophys. 172*, 135−142.
26. Guranowski, A., and Pawelkiewicz, J. (1977) *Eur. J. Biochem. 80*, 517−523.
27. Ueland, P. M., and Døskeland, S. O. (1977) *J. Biol. Chem. 252*, 677−686.
28. Palmer, J. L., and Abeles, R. H. (1979) *J. Biol. Chem. 254*, 1217−1226.
29. Schatz, R. A., Vunnam, C. R., and Sellinger, O. Z. (1979) in *Transmethylation* (Usdin, R., Borchardt, R. T., and Cleveling, C. R., Eds.) pp 143−153, Elsevier/North-Holland, New York, Amsterdam, and Oxford.
30. Fujioka, M., and Takata, Y. (1981) *J. Biol. Chem. 256*, 1631−1635.
31. Kajander, E. O., and Raina, A. M. (1981) *Biochem. J. 193*, 503−512.
32. Døskeland, S. O., and Ueland, P. M. (1982) *Biochim. Biophys. Acta 708*, 185−193.
33. Kim, I. K., Zhang, C. Y., Chiang, P. K., and Cantoni, G. L. (1983) *Arch. Biochem. Biophys. 226*, 65−72.
34. Hohman, R. J., Guitton, M. C., and Véron, M. (1984) *Arch. Biochem. Biophys. 233*, 785−795.
35. Shimizu, S., Shiozaki, S., Ohshiro, T., and Yamada, H. (1984) *Eur. J. Biochem. 141*, 385−392.
36. Hershfield, M. S., Aiyar, V. N., Premakumar, R., and Small, W. C. (1985) *Biochem. J. 230*, 43−52.
37. Porcelli, M., Cacciapuoti, G., Fusco, S., Iacomino, G., Gambacorta, A., De Rosa, M., and Zappia, V. (1993) *Biochim. Biophys. Acta 1164*, 179−188.
38. Ogawa, H., Gomi, T., Mueckler, M. M., Fujioka, M., Backlund, P. S., Aksamit, R. R., Unson, C. G., and Cantoni, G. L. (1987) *Proc. Natl. Acad. Sci. U.S.A. 84*, 719−723.
39. Kasir, J., Aksamit, R. R., Backlund, P. S., and Cantoni, G. L. (1988) *Biochem. Biophys. Res. Commun. 153*, 359−364.
40. Coulter-Karis, D. E., and Hershfield, M. S. (1989) *Ann. Hum. Genet. 53*, 169−175.
41. Sganga, M. W., Aksamit, R. R., Cantoni, G. L., and Bauer, C. E. (1992) *Proc. Natl. Acad. Sci. U.S.A. 89*, 6328−6332.
42. Kawalleck, P., Plesch, G., Hahlbrock, K., and Somssich, I. E. (1992) *Proc. Natl. Acad. Sci. U.S.A. 89*, 4713−4717.

43. Creedon, K. A., Rathod, P. K., and Wellems, T. E. (1994) *J. Biol. Chem. 269*, 16364−16370.
44. Palmer, J. L., and Abeles, R. H. (1976) *J. Biol. Chem. 251*, 5817−5819.
45. Gomi, T., Ishiguro, Y., and Fujioka, M. (1985) *J. Biol. Chem. 260*, 2789−2793.
46. Gomi, T., Date, T., Ogawa, H., Fujioka, M., Aksamit, R. R., Backlund, P. S., and Cantoni, G. L. (1989) *J. Biol. Chem. 264*, 16138−16142.
47. Gomi, T., Takata, Y., Date, T., Fujioka, M., Aksamit, R. R., Backlund, P. S., and Cantoni, G. L. (1990) *J. Biol. Chem. 265*, 16102−16107.
48. Aksamit, R. R., Backlund, P. S., Jr., Moors, M., Jr., Caryk, T., Gomi, T., Ogawa, H., Fujioka, M., and Cantoni, G. L. (1994) *J. Biol. Chem. 269*, 4084−4091.
49. Ault-Riche, D. B., Yuan, C. S., and Borchardt, R. T. (1994) *J. Biol. Chem. 269*, 31472−31478.
50. Yuan, C. S., Ault-Riche, D. B., and Borchardt, R. T. (1996) *J. Biol. Chem. 271*, 28009−28016.
51. Turner, M. A., Yuan, C. S., Borchardt, R. T., Hershfield, M. S., Smith, G. D., and Howell, P. L. (1998) *Nat. Struct. Biol. 5*, 369−376.
52. Otwinowski, Z., and Minor, W. (1997) *Methods Enzymol. 276*, 307−326.
53. Takusagawa, F. (1992) *J. Appl. Crystallogr. 25*, 26−30.
54. Matthews, B. W. (1968) *J. Mol. Biol. 33*, 491−497.
55. Brünger, A. T. (1993) *X-PLOR 3.1: A system for X-ray crystallography and NMR*, Yale University Press, New Haven and London.
56. Brünger, A. T. (1990) *Acta Crystallogr. A46*, 46−57.
57. Lamzin, V. S., Dauter, Z., Popov, V. O., Harutyunyan, E. H., and Wilson, K. S. (1994) *J. Mol. Biol. 236*, 759−785.
58. Jones, T. A. (1985) *Methods Enzymol. 115*, 157−171.
59. Cambillau, C., and Horjales, E. (1987) *J. Mol. Graphics 5*, 174.
60. Brünger, A. T. (1992) *Nature 255*, 472−474.
61. Laskowski, R. A., MacArthur, M. W., Moss, D. S., and Thornton, J. M. (1993) *J. Appl. Crystallogr. 26*, 283−291.
62. Cheng, X., Kumar, S., Posfai, J., Pflugrath, J. W., and Roberts, R. J. (1993) *Cell 74*, 299−307.
63. Vidgren, J., Svensson, L. A., and Liljas, A. (1994) *Nature 368*, 354−356.
64. Labahn, J., Granzin, J., Schluckebier, G., Robinson, D. P., Jack, W. E., Schildkraut, I., and Saenger, W. (1994) *Proc. Natl. Acad. Sci. U.S.A. 91*, 10957−10961.
65. Reinisch, K. M., Chen, L., Verdine, G. L., and Lipscomb, W. N. (1995) *Cell 82*, 143−153.
66. Gong, W., O'Gara, M., Blumenthal, R. M., and Cheng, X. (1997) *Nucleic Acids Res. 25*, 2702−2715.
67. Hodel, A. E., Gershon, P. D., Shi, X., and Quiocho, F. A. (1996) *Cell 85*, 247−256.
68. Fu, Z., Hu, Y., Konishi, K., Takata, Y., Ogawa, H., Gomi, T., Fujioka, M., and Takusagawa, F. (1996) *Biochemistry 35*, 11985−11993.
69. Djordjevic, S., and Stock, A. M. (1997) *Structure 5*, 545−558.
70. Bussiere, D. E., Muchmore, S. W., Dealwis, C. G., Schluckebier, G., Nienaber, V. L., Edalji, R. P., Walter, K. A., Ladror, U. S., Holzman, T. F., and Abad-Zapatero, C. (1998) *Biochemistry 37*, 7103−7112.
71. Dreusicke, D., Karplus, P. A., and Schulz, G. E. (1988) *J. Mol. Biol. 199*, 359−371.
72. Wierenga, R. K., Terpstra, P., and Hol, W. G. J. (1986) *J. Mol. Biol. 187*, 101−107.
73. Gomi, T., and Fujioka, M. (1984) *Biochim. Biophys. Acta 785*, 177−180.
74. Bennett, W. S., Jr., and Steitz, T. A. (1978) *Proc. Natl. Acad. Sci. U.S.A. 75*, 4848−4852.
75. Henderson, R., Baldwin, J. M., Ceska, T. A., Zemlin, F., Beckmann, E., and Downing, K. H. (1990) *J. Mol. Biol. 213*, 899−929.
76. Pebay-Peyroula, E., Rummel, G., Rosenbusch, J. P., and Landau, E. M. (1997) *Science 277*, 1676−1681.
77. Doyle, D. A., Cabral, J. M., Pfuetzner, R. A., Kuo, A., Gulbis, J. M., Cohen, S. L., Chait, B. T., and MacKinnon, R. (1998) *Science 280*, 69−77.
78. Cowan, S. W., Schirmer, T., Rummel, G., Steiert, M., Ghosh, R., Pauptit, R. A., Jansonius, J. N., and Rosenbusch, J. P. (1992) *Nature 358*, 727−733.
79. Malone, T., Blumenthal, R. M., and Cheng, X. (1995) *J. Mol. Biol. 253*, 618−632.
80. Takusagawa, F., Kamitori, S., and Markham, G. D. (1996) *Biochemistry 35*, 2586−2596.
81. Dixon, M. M., Huang, S., Matthews, R. G., and Ludwig, M. (1996) *Structure 15*, 1263−1275.
82. Rafferty, J. M., Somers, W. S., Saint-Girons, I., and Phillips, S. E. V. (1989) *Nature 341*, 705−710.
83. Turner, M. A., Dole, K., Yuan, C. S., Hershfield, M. S., Borchardt, R. T., and Howell, P. L. (1997) *Acta Crystallogr. D53*, 339−341.

BI990332K